LABORATORI NAZIONALI DI FRASCATI
SIS-Pubblicazioni

LNF-01/028 (IR)
13 Novembre 2001

MEASUREMENTS OF MAGNETIC FIELD IN THE PROTOTYPE OF THE OPERA SPECTROMETER

G. Di Iorio[1,2], B. Dulach[1], M. Incurvati[1,3], M. Spinetti[1], F. Terranova[1], L. Votano[1]
[1)] *INFN, Laboratori Nazionali di Frascati, Frascati, Italy*
[2)] *Dip. Scienze Fisiche, Univ. di Napoli, Napoli, Italy*
[3)] *Dip. Ingegneria Elettrica, Univ. "La Sapienza", Roma, Italy*

Abstract

Measurements of magnetic fields in the prototype of the OPERA spectrometer are reported. Both the magnetic flux B in the iron and the fringe field in air have been measured by means of pick up coils and Hall probes. These measurements are aimed to the determination of the value of B in the bulk of the spectrometer for different currents and test the magnetic properties of the material in a full-scale prototype. Moreover, comparisons with simulations based on finite-element analysis have been carried out.

PACS:14.60Pq, 07.55Db

1 Introduction

A prototype of spectrometer has been built in Frascati to test the mechanics and magnetic properties of the warm iron dipolar magnet foreseen for the OPERA experiment [1]. A full description of the prototype can be found elsewhere [2]; this note describes the techniques employed to measure the magnetic field in iron and demonstrates that the nominal fields considered in the proposal can be achieved, as expected, with a current of about 55000 Ampere·turns. Furthermore, field uniformity has been tested in the sensitive region of the magnet and compared with simulation.

2 The prototype

The prototype of the OPERA dipolar magnet (Fig.1) consists of two vertical walls of rectangular cross section and of top and bottom flux return path. The walls are built lining four iron layers (5 cm think) interleaved with 2 cm of air allocated for the housing of RPC. Each iron layer is made up of two plates $50 \times 1250 \times 8200$ mm^2. The final OPERA spectrometer is supposed to have the same structure but will be made up of seven plates instead of two (overall length 8750 mm) and 12 layers instead of 4 [1]. The final dipole will be magnetized by means of two coils, 23 turns each, installed in the top and bottom flux return path. The nominal current flowing in the coils is 1200 A, corresponding to an overall magnetomotive force of 55200 Ampere·turns. However, at present, only one copper coil (23 turns) has been installed in the bottom plane of the prototype. The upper plane is equipped with a second coil made of flexible 26 mm diameter copper wire. The maximum current that can flow in this conductor is about 600 A. Therefore, in the prototype the maximum magnetomotive force is just 27600 A-turns (600 A $\cdot$ 23 turns $\cdot$ 2 coils) if the two coils are connected in series with a single power supply. The nominal field has been reached installing a further couple of coils in the central part of the dipole. Clearly, this configuration can be used only to test the maximum field achievable since it spoils the field uniformity along the dipole height. Field uniformity measurements have been done with a lower value of current using the top and bottom coils with a current of about 600 A.

3 The experimental apparatus

Most of the measurements have been done installing pick up coils along the dipole. A fixed coil consisting of a conduction wire wound in one of the vertical wall at a height of 2.34 m from the floor has been used to test the maximum available field and the magnetic properties of the material. A removable 25-turn coil built from a flat cable has been

Figure 1: The OPERA dipolar magnet prototype.

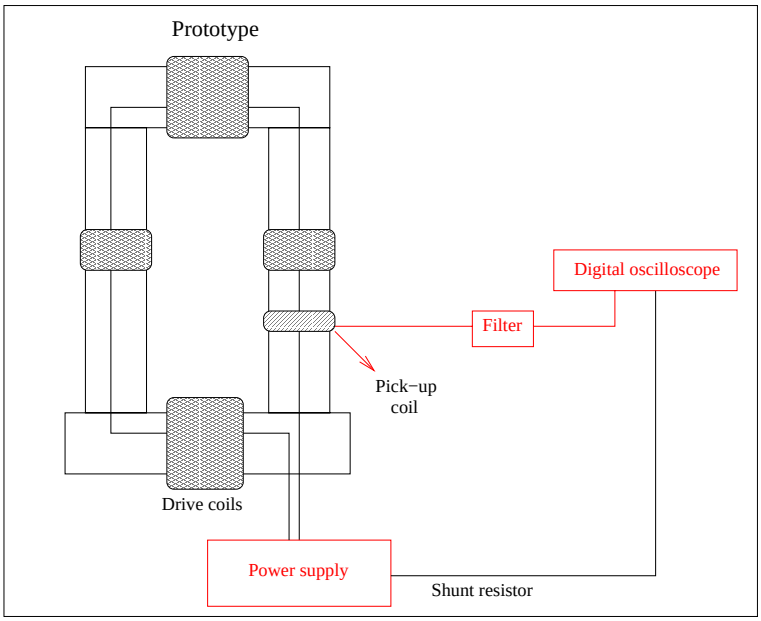

Figure 2: Sketch of the experimental apparatus

used for the measurement of field uniformity. The end-point of the coils are connected to a coaxial cable. The signal is, then, filtered and sent to a digital oscilloscope. The oscilloscope, hence, acts as a voltmeter, recording the induced voltage at the two end of the coil as a function of time. The integration is performed off-line. The power supply is a Danfysik System 8000 (maximum power: 132 kW). The current ramp speed di/dt is approximately constant and depends on the load impedance. It can be varied up to a factor two by means of a potentiometer. It has been precisely monitored recording the shunt voltage from the power supply in a separate channel of the oscilloscope. The trigger for the scope is provided manually. The apparatus is shown schematically in Fig.2.

The measure of the magnetic flux B is based on the voltage induced in the pickup coil during the ramp-up (ramp-down) of the power supply ("ballistic measurement"). The variation of the current flowing in the drive coils induces a change in the magnetic flux cut by the pickup coil; the induced voltage is

$$V_i = -\frac{d\Phi(t)}{dt} = -\frac{d}{dt}\int_S \vec{B}(t)\cdot\vec{n}\,ds = -SN\frac{d}{dt}\langle B\rangle(t) \tag{1}$$

and integrating:

$$\frac{-1}{SN}\int_0^t dt' V_i(t') = \frac{1}{SN}(\Phi(t)-\Phi(0)) = \Delta\langle B\rangle(t) \tag{2}$$

where S is the cross sectional area of one turn of the pickup coil, N is the number of turns and $\Delta\langle B\rangle$ is the increase of magnetic field going from $t'=0$ to $t'=t$ averaged in

each point of the surface of the turn S. In particular, if $B(t'=0)=0$ (no residual field) eq.2 gives just the average magnetic field in the bulk of iron. In our case the turns cut a region in space containing both the iron slabs and the air. Since $B_{iron} \gg B_{air}$ and the cross sectional area of the turn in iron is of the same order of the one in air ($S_{iron} \simeq S_{air}$), in most of our measurements the latter can be safely neglected and eq.2 provides directly the average increase of field *in iron* if $S = S^{iron}$, i.e.

$$\Phi = N \int_S \vec{B} \cdot \vec{n}\, ds = N \left(\int_{S^{iron}} \vec{B}_{iron} \cdot \vec{n}\, ds + \int_{S^{air}} \vec{B}_{air} \cdot \vec{n}\, ds \right) \simeq$$

$$N \int_{S^{iron}} \vec{B}_{iron} \cdot \vec{n}\, ds \;=\; \langle B \rangle \cdot N S^{iron}$$

The shape of the function $V_i(t)$ is driven by the strong nonlinear behavior of ferromagnetic materials. Even in the ideal case ("toroidal approximation"), a constant di/dt does not imply a constant induced voltage:

$$V_i = -SN \frac{d}{dt}(\mu(H) \cdot H) = -SN \frac{d}{dt}(\mu(ni) \cdot ni) =$$
$$-SNn \left[\frac{d\mu}{di} \frac{di}{dt} i(t) \;+\; \mu(ni(t)) \frac{di}{dt} \right]$$

being H the magnetic intensity, $\mu(H)$ the magnetic permeability of iron and n the number of driving turns per unit length ($B = \mu H = \mu ni$). Hence, also in the occurrence of $di/dt = const$, a non-constant $V_i(t)$ is observed unless

$$\left[\frac{d\mu}{di} i(t) \;+\; \mu(i(t)) \right] = const \tag{3}$$

which, in general, does not hold for each i in ferromagnetic materials.

4 Magnetic properties of iron

Three small toroids (11.4 cm outer diameter) have been built with iron belonging to the same heat as the one of the prototype. A set of hysteresis curves for these samples have been measured for various magneto-motive forces. Figure 3 shows the curves for $H_{max} = 209, 403, 806, 1612$ and 2418 A/m [1]. Figure 4 represents the hysteresis in the saturation regime. It is worth noticing that the actual spectrometer is supposed to work with a

[1] These measurements have been performed at CERN by G.Peiro from the LHC/MMS division. The currents were chosen to ease the comparison with Table 1 and correspond approximately to the A-turns of that table as far as the approximation $H = ni$ holds for the prototype ($n = 4.7619\ \mathrm{m}^{-1}$).

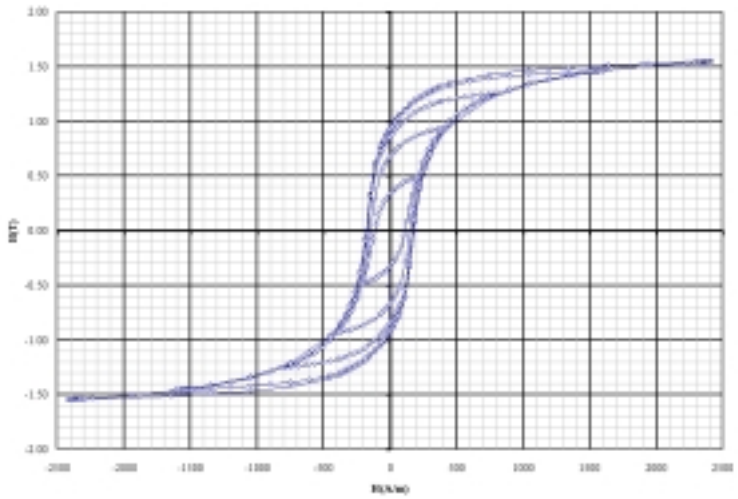

Figure 3: Hysteresis curve for the sample toroid at $H_{max} = 209, 403, 806, 1612$ and 2418 A/m.

magneto-motive force $Ni = 55200$ A-turns, corresponding to $H_{max} \simeq 2852$ A/m. In this regime ($H_{max} \simeq 2000 - 3000$ A/m) the value of B_{max} is not fully saturated but the residual field at $H = 0$ is very stable, due to the full orientation of the Weiss domains. In the toroidal sample it is about $B_r = 0.9$ T. The maximum increase of field that can be achieved by magneto-motive forces is $B_{max} - B_r \simeq 0.85$ T (see Fig.4), the coercive force H_c is about 180 A/m. Finally, the first magnetization curve is depicted in Fig.5.

5 Non-static measurements of magnetic field

5.1 Estimate of B

Measurements of the hysteresis curves are used to be performed in "quasi-static" conditions i.e. with very low values of di/dt or even increasing the current in short bursts and keeping i constant between the bursts to allow for relaxation of the Weiss domains. The power supply in our disposal was not well-suited for this kind of measurement being di/dt quite large and poorly adjustable. We will discuss in the next session how to overcome this limitation and obtain a hysteresis curve also for the full-size prototype. On the other hand, non-static measurements can be safely used to measure the increase of field between two points, as far as the integration of the induced voltage extends beyond the time when the power supply reaches the maximum current value to account for relaxation. In this case

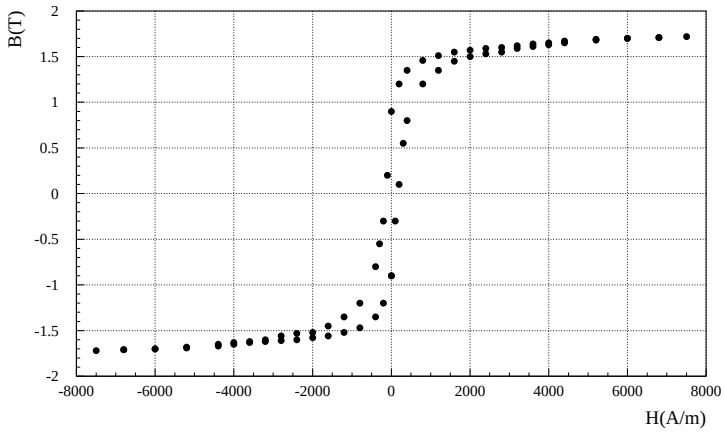

Figure 4: Hysteresis curve for the sample toroid in saturation regime.

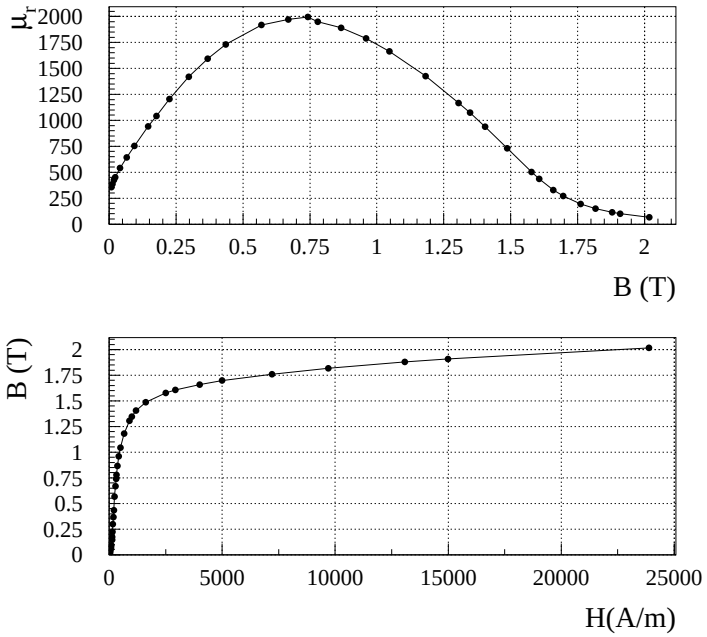

Figure 5: Magnetic permeability of iron versus B (top plot) and B-H curve (bottom plot) during the first magnetization after full degaussing.

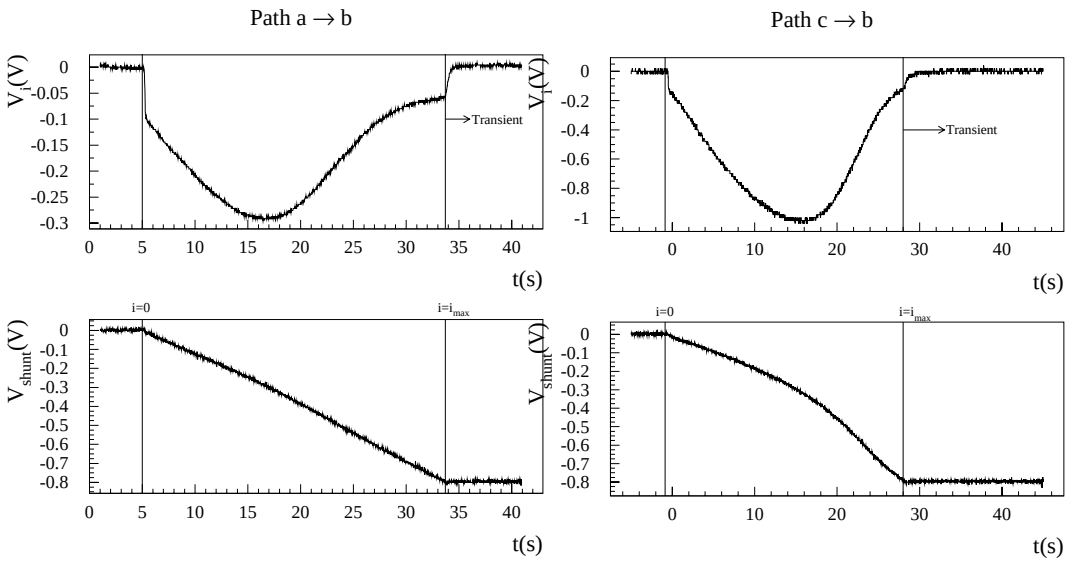

Figure 6: Induced voltage (upper plot) and shunt voltage (lower plot) going from 0 to 368 A for two different paths along the hysteresis curve

$$\int_0^\infty dt\, V_i(t) \;=\; -(\Phi_{fin} - \Phi_0) = \frac{-1}{SN}(\langle B\rangle_{fin} - \langle B\rangle_0) \tag{4}$$

where the subscript *"fin"* indicates the value reached for $t \to +\infty$, i.e. when the power supply provides a current $i = i_{max}$ and the transient due to relaxation is faded out. As a purpose of illustration Fig.6 shows the induced voltage in the pick-up coil when the current in the four 23-turn drive coils goes from zero to 368 A and $B_r = B_0 > 0$ (path $a \to b$ of Fig.7-left) or $B_r = B_0 < 0$ (path $c \to b$ of Fig.7-left) [2].

During these measurements we tried to perform a complete degaussing of the prototype. In particular we performed hysteresis cycles decreasing smoothly H_{max} and computing the maximum field obtained for each H_{max} in the region covered by the pick-up coil. The results are plotted in Figg.8 and 9. All points were obtained with 4 drive coils, each consisting of 23 turns. The plot of Fig.8 shows the values obtained cycling around several hysteresis curve (each characterized by its own H_{max} or, as in our plot, $N \cdot i_{max}$); the Fig.9 represents the best estimate of the magnetic field B at the pick-up coil and it is compared with the results of the simulation based on the TOSCA code (see Appendix). The ratio data/simulation is plotted in Fig.10. In each cycle we performed four measurements: we computed ΔB going from c to b (path 1 of Fig.7 right), from b to a (path 2),

[2]The basic unit of the power supply is 92 A, so in this case we set a current increase of four units. It corresponds to a ΔV of 800 mV across the shunt resistor (200 mV$\equiv$ 92 A).

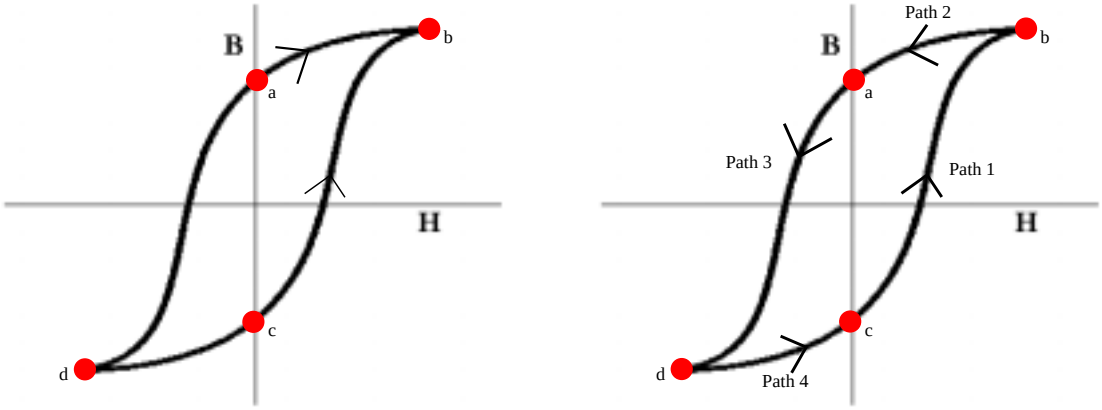

Figure 7: Paths for Figg.6 (left) and 8 (right)

from a to d (path 3) and from d to c (path 4). Each cycle provides two estimates of B: $(\Delta B_1 + \Delta B_4)/2$ and $(\Delta B_2 + \Delta B_3)/(-2)$. All the estimates can be found in Table 1 (in Fig.8 the average of the two is plotted).
A few remarks are in order:

- As expected, the residual field stays constant in a wide range of $N \cdot i_{max}$ above a certain threshold. Beyond this threshold, all the Weiss domains choose their direction of easy-magnetization (EMD) closest to the direction of H. In this case an increase of H_{max} does not induces a change of EMD (and, hence, an increase of B_r) but just rotate the EMD closer to H, increasing B_{max} . This effect vanishes when $H = 0$ and all the Weiss domains get back their EMD.

- A consistency check is the closure of the path along the hysteresis curves $\gamma(H_{max})$:

$$\oint_{\gamma(H_{max})} d\vec{B} = \Delta B_1 + \Delta B_2 + \Delta B_3 + \Delta B_4 = 0 \qquad (5)$$

  Eq.5 can be compared with the measured values directly from Fig.8. It is worth noticing that for $i_{max} < 184$ A, B_r changes drastically going from one $\gamma(H_{max})$ to another and, in order to stabilize the path, it is always advisable to cycle several times along the same γ before performing the measurement. Here, the dipole was cycled only once before the measurement because the procedure is extremely time-consuming with the present apparatus. This is probably enough for the current sensitivity of the apparatus, since the observed mismatch in the measured value of eq.5 is compatible with the experimental uncertainty.

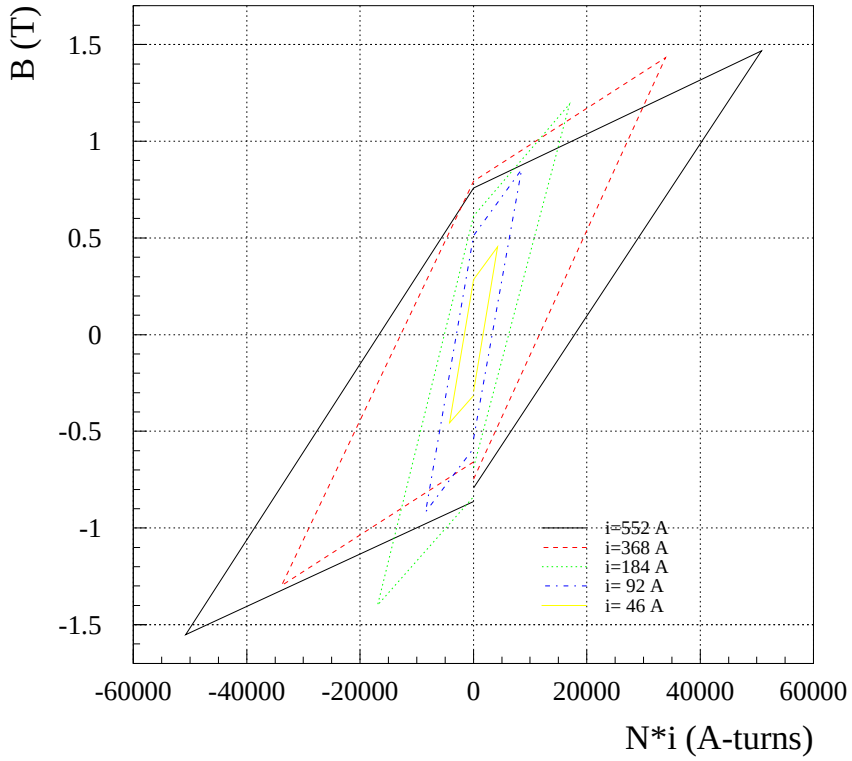

Figure 8: Measured values of ΔB for different hysteresis cycles.

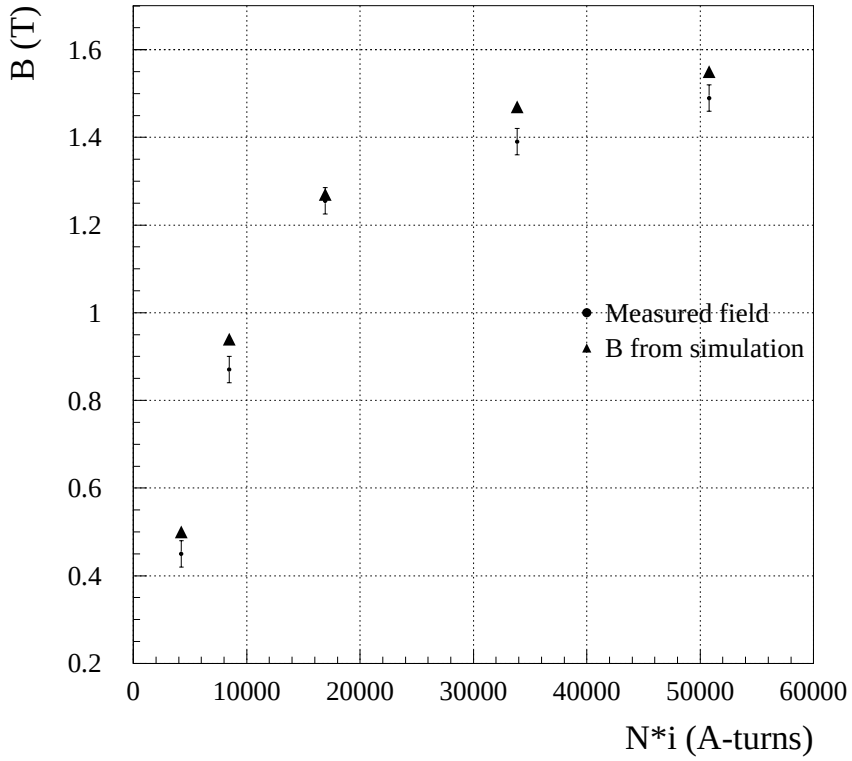

Figure 9: Field at the pick-up coil versus current.

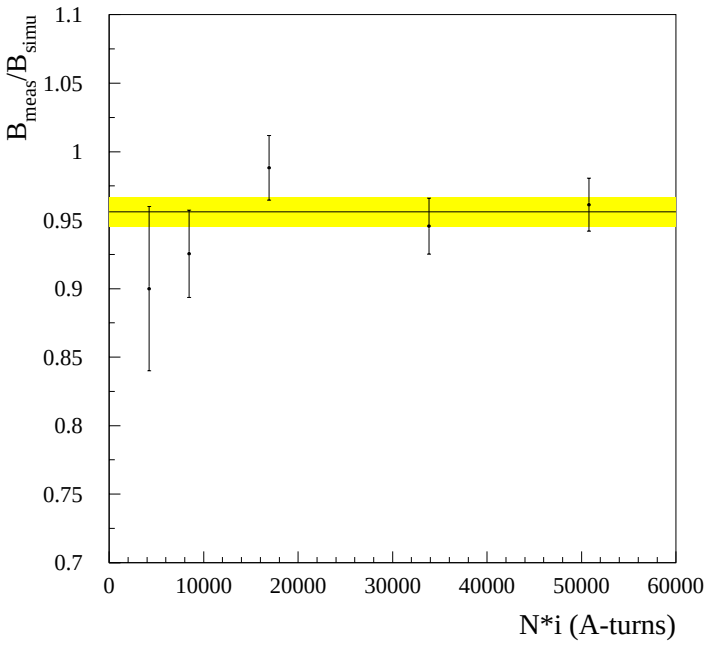

Figure 10: Ratio measured/predicted field at the pick-up coil versus current.

5.2 Experimental errors

The main sources of error are related with the integration of V_i. In particular, baseline fluctuations and environmental background represent a non negligible contribution since the integration is performed for time intervals of the order of several tenths of seconds. During the studies of field uniformity (see sect.7), the apparatus was set in such a way that it has been possible to acquire simultaneously the voltage at the fixed pick-up coil and the induced voltage at the mobile one. Hence several measurements of the same quantity has been collected and experimental errors have been estimated (see Fig.11).

Systematics have been investigated performing measurements with different di/dt and with $di/dt = 0$ ("empty measurements" for signal to noise evaluation). No significant biases were found apart from an increase of environmental e.m. noise correlated with the start-up of DAFNE after the summer shutdown [3].

[3]The prototype is currently located in the former KLOE mounting hall, very close to the DAFNE accelerator.

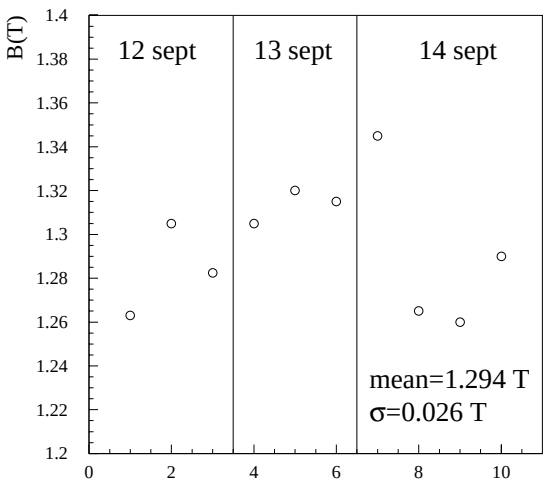

Figure 11: B at the fixed coil with $i = 598$ A

Current (A-turns)	B from $d \to c \to b$ (Tesla)	B from $b \to a \to d$ (Tesla)	Average (Tesla)
4232	0.45	0.45	0.45
8464	0.89	0.86	0.875
16928	1.29	1.22	1.255
33856	1.37	1.41	1.39
50784	1.51	1.47	1.49

Table 1: Estimate of B at the pick-up coil from path $b \to d$ and $d \to b$.

6 Magnetic properties of the material

The knowledge of the magnetic properties of the steel, in particular the set of B-H curves, is an important input for the simulation of the dipole. The curves have been precisely measured using a toroidal sample of the same steel, as described in sec.4. It is advisable to cross-check that the stresses and deformations of the steel in the full-size prototype do not modify substantially these properties. In general, differences between the prototype and the small toroids are expected, especially in the residual field and in B_{max}, due to the presence of sharp angles and air gaps. From the experimental point of view, the measurement strictly requires a quasi-static regime. To extract the hysteresis curve for each value of H, eq.2 is used *not only* for $t \rightarrow +\infty$. Each point of the experimental BH-curve is defined by the pair:

$$\begin{cases} H(t) = & n \cdot i(t) \\ B(t) = & \frac{-1}{SN} \int_0^t dt' V_i(t') \ + \ B(t=0) \end{cases}$$

where n is the total number of turns divided by the overall length of the magnetic circuit [4]. If i changes too rapidly, the Weiss domains cannot relax and $B(t)$ is underestimated until $t \rightarrow +\infty$. The lower the speed di/dt, the higher the measured value of B. As noted before, the present setup is ill-suited for this kind of measurement because the ramp of the power supply cannot be decreased below 6.5 A/s. In order to evade this limitation, a multistep ramp has been implemented. During these measurements the current was increased (or decreased) eight times of a value $i_{max}/8$. The steps were separated by time intervals of 5 s to allow (at least partially) for relaxation. Afterwards, the hysteresis curve was interpolated using just the 8 H-B pairs obtained after each relaxation (see Fig.12). The results obtained for $i_{max} = 368$ A ($H_{max} = 1752$ A/m in the approximation $H = ni$) are plotted in Fig.13. This curve is in reasonable agreement with Fig.3 at $H_{max} = 1612$ A/m especially for what concerns B_{max} (apart from the above-mentioned deficit) and the coercivity H_r. The value of B_r is about 0.1 T smaller than the one measured with the toroidal sample. The use of the multiramp technique solved the problem of an apparent widening of the curve observed with a constant di/dt of 6.5 A (see Fig.14) even if, as can be inferred from Fig.12, a 5 s inter-burst is still slightly too short [5].

[4] Strictly speaking, the linear relation between the magnetic intensity and the magneto-motive force $H = n \cdot i$ holds only for simple geometries, like the toroid. Here it should be considered as an approximation.

[5] It was not possible to further increase the integration time, due to the limited size of the buffer of the oscilloscope.

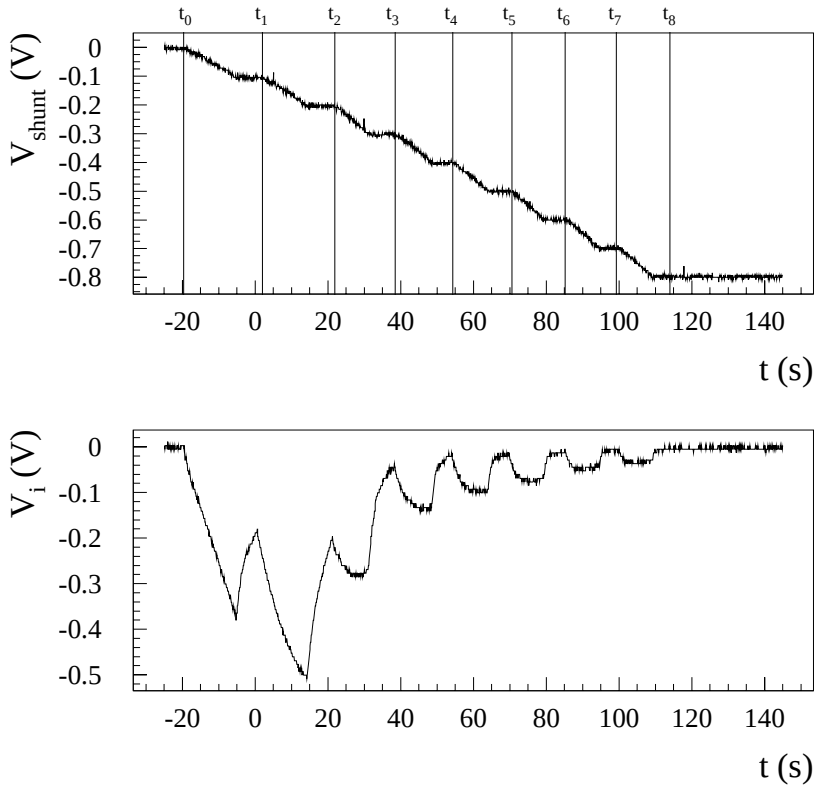

Figure 12: Shunt and induced voltage during a multistep ramp of the power supply. The vertical lines show the points used for the interpolation of the BH-curve. The data refer to ΔB_1 (path 1) at $i_{max} = 368$ A.

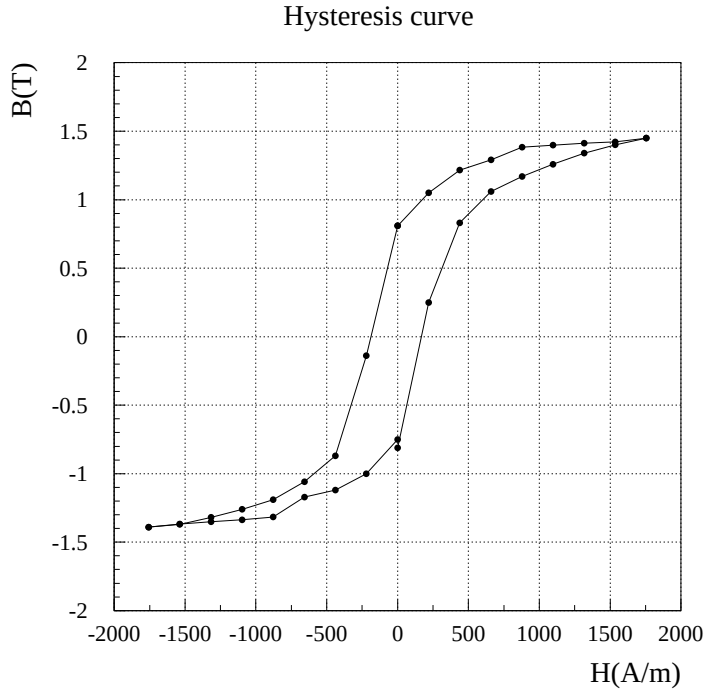

Figure 13: Hysteresis curve for the prototype at $i_{max} = 368$ A.

7 Field uniformity

The tests of field uniformity were carried out connecting only the upper and lower coils to the power supply, as foreseen for the final OPERA dipole. However, the present apparatus does not allow a test of field uniformity with nominal currents, since it is not possible to run with more than $\sim$600 A flowing in the coils. Hence the current was set to 598 A, corresponding to an overall magneto-motive force of 27508 A-turns. Two set of measurements have been recorded. The first set is done winding the mobile coil around one of the column of the prototype at different heights, hence averaging over the four slabs. Hereafter, the coil has been positioned at fixed height (2.34 m) and wound around one single slab in order to test non-uniformities among the four slabs making up the column. Each measurement consists of a full hysteresis cycle at $i = 598$ A. During the data taking also the fixed coil positioned at 2.34 m has been acquired in a different channel of the oscilloscope. The purpose is twofold: when the mobile coil is positioned at the same height, it can be checked that no systematic related with the use of different coils biases the measurement; moreover, during the whole test many measurements of the same field were done, allowing an estimate of the (statistical) error on B and checking stability in

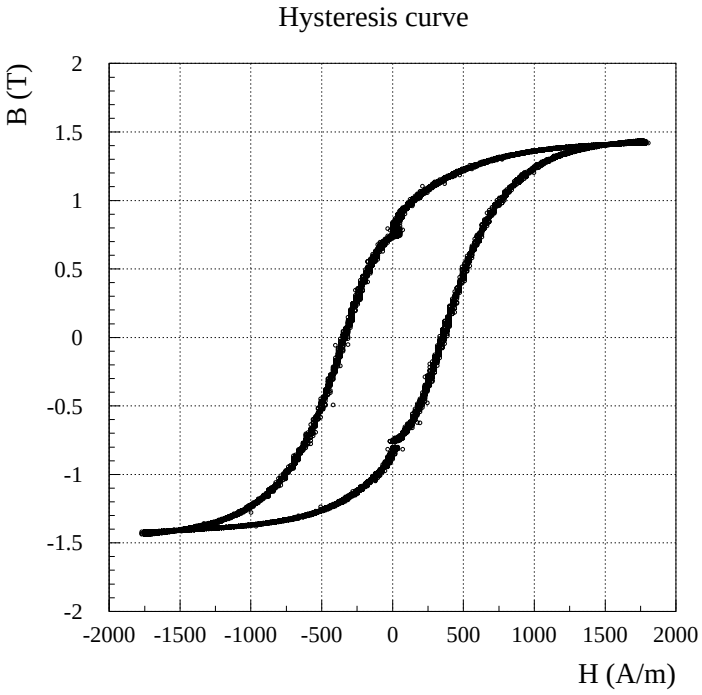

Figure 14: Hysteresis curve for the prototype at $i_{max} = 368$ A but with constant velocity di/dt=6.5 A.

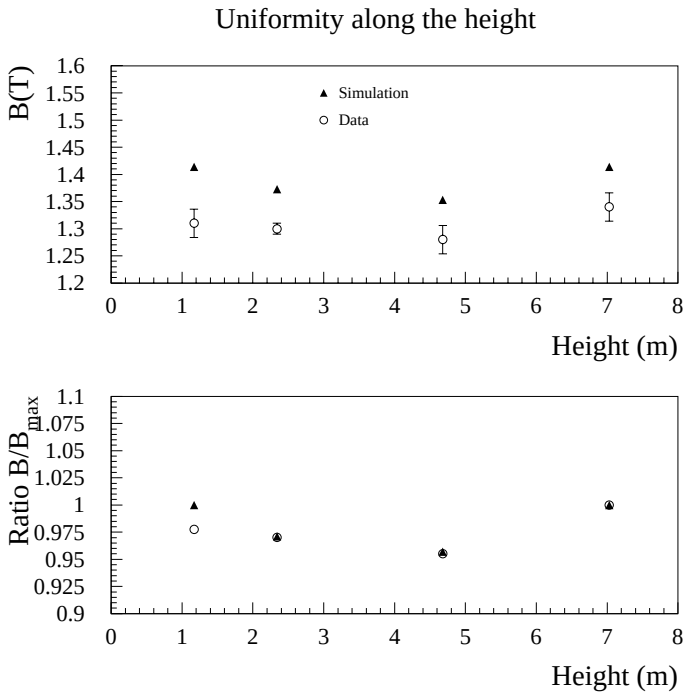

Figure 15: B versus height.

time as discussed in sec.5.2.

Fig.15 shows the B field at different heights in one column of the magnet in absolute (upper) and relative (lower) scale. Comparison with TOSCA is also shown. The B field along the slab at fixed height is shown in Fig.16.

Non-uniformities in height do not exceed 5%, in agreement with the specifications done at the level of proposal and with simulation. On the other hand, as already pointed out in sec.5, a systematic deficit of field of about 4% is observed with respect to TOSCA results. In particular, Fig.16 points toward a deficit mainly due to the external slabs. Possible explanations are either magnetic short-circuits below the floor or poor mechanical contact of some of the slabs with the top iron block. This effect will be discussed further in sec.9.

8 Fringing field

A map of fringing field in air is a useful piece of information and complements the absolute calibration performed by the pick-up coils. Measurements of field in the surrounding air or in small gaps could be used to monitor the relative variation in time during the

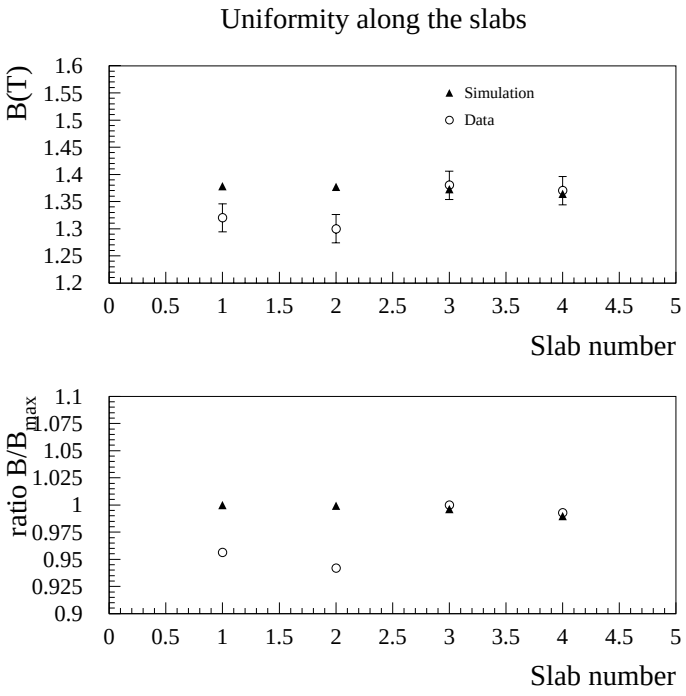

Figure 16: B at different slabs at 2.34 m height.

OPERA data taking and, combined with finite-element calculation, can provide information on possible losses of magnetic flux. Measurements have been performed by means of Hall probes during the test of field uniformity (two-coil configuration at $i = 598$ A). In particular, the field in air in the gaps between the slabs has been recorded at different heights. Fig.18 shows the value of $|B|$ and of its component along the vertical direction (B_z) versus height. The first two plots refer to the rightmost gap with respect to the driving coil (gap "a" of Fig.17), the second pair to the middle gap (gap "b") and the third to the gap closest to the coil (gap "c"). The measurement of the field in air in the region surrounding the column (zone "d" of Fig.17) has been found particularly interesting, since the systematic excess of horizontal field (labeled B_x) is an indication of unexpectedly high dispersed flux and is probably connected with the systematic deficit of the bulk field in iron compared with TOSCA (see Fig.19).

9 Deficit of magnetic flux

The measurements recorded from the pick-up coils provide indication of a small deficit (of the order of 4% - see Fig.10) with respect to TOSCA. This effect is not relevant for

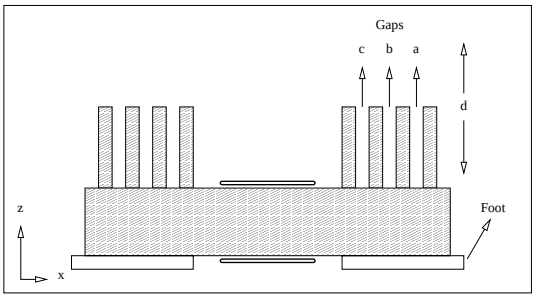

Figure 17: Air gaps where B has been measured.

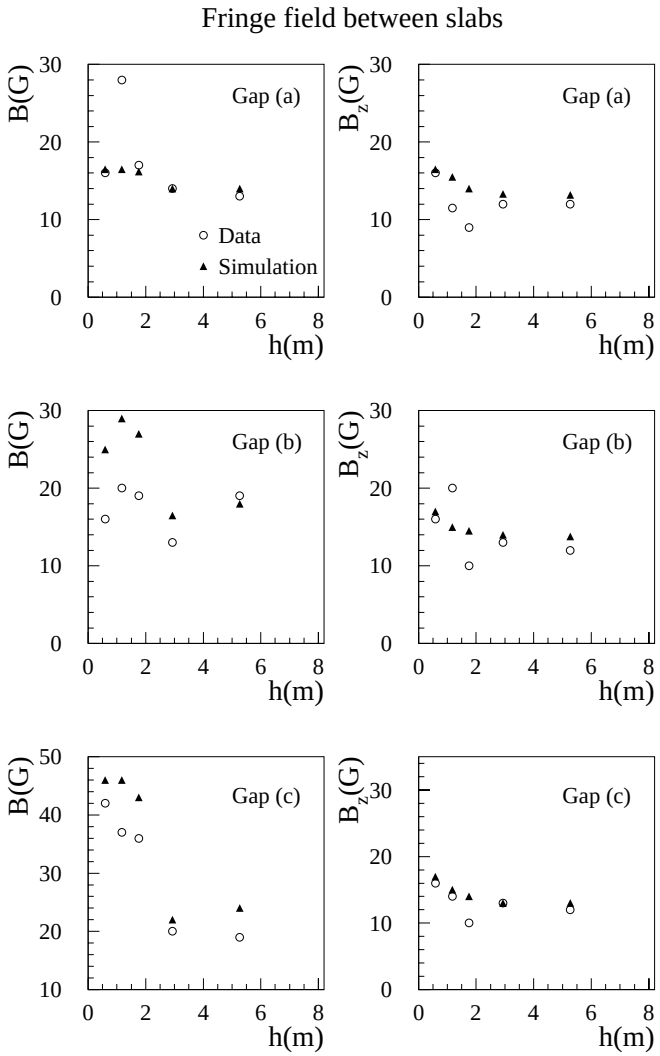

Figure 18: Magnetic field (in Gauss) in the gaps versus height.

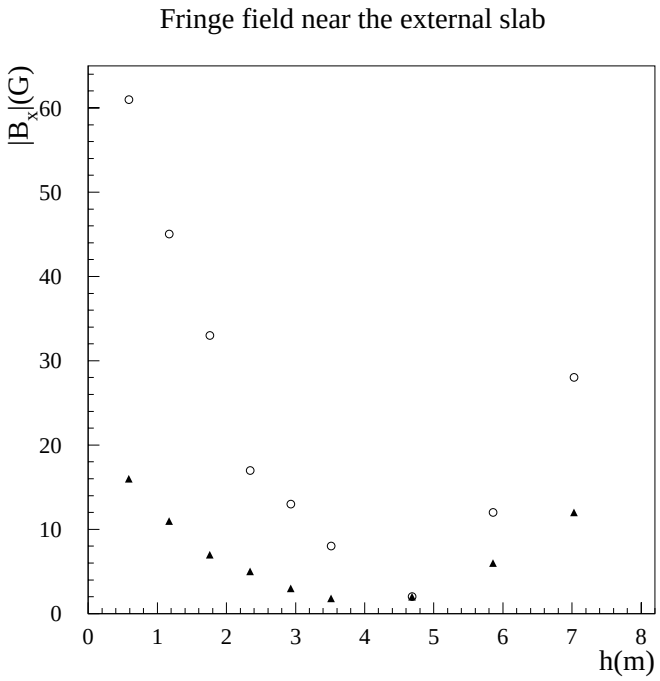

Figure 19: Magnetic field (in Gauss) 10 cm far from the rightmost slab versus height.

the physics performance of the spectrometer; moreover, if needed, in the final dipole part of the field can be recovered increasing the current through the driving coils. On the other hand, the effect has not a straightforward explanation. Air gaps between the vertical slabs and the top return path due to poor mechanical contact are unlikely to explain the whole deficit. To show this, it is enough to employ the linear relationship between magneto-motive force and flux (Hopkinson's law):

$$Ni = \mathcal{R}\Phi$$

which, as far as $\mathcal{R}$ does not depend on Φ (small perturbation of the nominal field), is formally equivalent to the Ohm's law. Hence the prototype can be treated as an ordinary linear circuit with two ideal power supplies as the one in Fig.20-a. Here R_{slab} is the reluctance of the slab, $R_{top} = R_{bottom}$ are the reluctances of the return path and $\Delta V = Ni$. The measured tolerance between the slab and the ceiling of the dipole does not exceed 0.2 mm. Even in the worse case this corresponds to a reluctance in series with at most three slabs as shown in Fig.20-b. Solving the circuit, a deficit of no more that 1.4% is found at $598\ A$. However, the effect could be amplified by the fact that the top and bottom return paths are made up of four horizontal slabs, one upon the other solded just at the

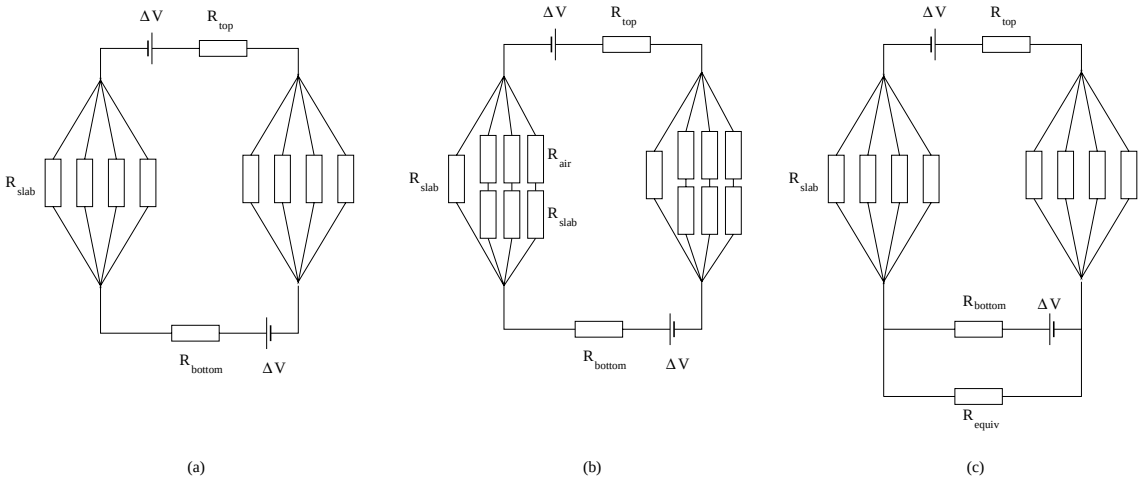

Figure 20: Resistive equivalent of the dipole.

external border, giving rise to additional air gaps. It is interesting to note that the return path of the final spectrometer is homogeneous and this effect will not contribute anymore at Gran Sasso.

Finally, the prototype is fixed to ground by means of steel nails (∅=3 cm). They are partially in contact with the ground mesh of the hall which is made up of 2.6 cm diameter iron wires forming a frame of 20×20 cm^2 buried 3 cm below the floor. Nails and the iron frame surrounding the concrete feet of the dipole can short-circuit the magnetic path as shown in Fig.20-c. Clearly, a detailed simulation of this effect is impractical, however an estimate of the corresponding reluctance and of the expected flux at each "foot" (see Fig.17) can be drawn solving simultaneously the circuits of Figg.20-a and 20-c and imposing the ratio of the fluxes in the vertical wall to differ of about 4%. The expected flux is about 0.50 Vs. A measurement of the flux in the "foot" has been performed, resulting in $\Phi \leq 0.05$ Vs. Hence, strong short-circuits through the nails and the iron frame are excluded. Again, it is worth noticing that any contribution coming from this effect will disappear in the Gran Sasso hall, where no iron grid has been installed below the floor at a depth lower than 50 cm.

10 Conclusions

A systematic study of the magnetic properties of the OPERA dipole prototype has been carried out. Measures of the field in the bulk of the spectrometer have been done employing the "ballistic method" and installing pick-up coils along the spectrometer. Additional information have been extracted by Hall probes recording the fringing field in air. It turns out that the choice of the iron is appropriate to reach the nominal field and its magnetic

properties are not modified by mechanical stresses. The non-uniformity of the field along the height does not exceed 5% in agreement with specifications. An average 4 ± 1 % deficit of magnetic flux is observed with respect to simulations made assuming ideal mechanical contact and complete isolation of the dipole from the hall.

11 Acknowledgments

We are greatly indebted to the Electrotechnics Group of the LNF Accelerator Division and in particular to F. Iungo, C. Sanelli, F. Sardone for the installation of the power supply and for support during the measurements. G. Peiro (LHS/MMS division of CERN) performed all the tests concerning the small sample toroids. A special thank to A. Cecchetti, M. Ventura and S. Mengucci, G. Paoluzzi and G. Papalino for preparing and installing the coils. We are also indebted with J. Billan, G. Corradi, M. Losasso, J. Nelson, P. Negri and A. Para for many useful discussions.

Appendix: Simulation of the spectrometer

A detailed simulation of the dipole magnetization is of utmost importance to model non-uniformities of the field in the sensitive region of the spectrometer and fine-tune the algorithms for the reconstruction of particle trajectories and momenta. By far the most common technique used to solve Maxwell equations in the steady current regime in presence of non-linear materials is the Finite Element method. In particular, the 3-D solver TOSCA [3] has been employed for this analysis. A comprehensive description of the simulation of the OPERA spectrometer can be found elsewhere [2]. Here the main features and results for the prototype are recalled.

In TOSCA, the magnet is modeled by defining its geometry in a base plane and then extruding that geometry into the third dimension. The materials considered for the spectrometer are a non-linear steel making up the bulk of the magnet, ideal conductors (the drive coils) and air. TOSCA is not able to deal with hysteresis phenomena and requires a uniquely defined BH-curve. Moreover, solutions of the Maxwell equations are provides only for the static regime and TOSCA is by no means intended for simulation of the time-evolution of ballistic measurements but computes precisely the fields at $t \to +\infty$. The BH-curve has been drawn from the measurements of the sample toroids (see e.g. Fig.5).

The model used in the prototype is shown in Fig.21. Fig.22 shows the magnetic field at the center of the pick-up coil in the four vertical slabs (the current is $i = 552$ A with 4 drive coils). The field in iron varies by less than 0.5%.

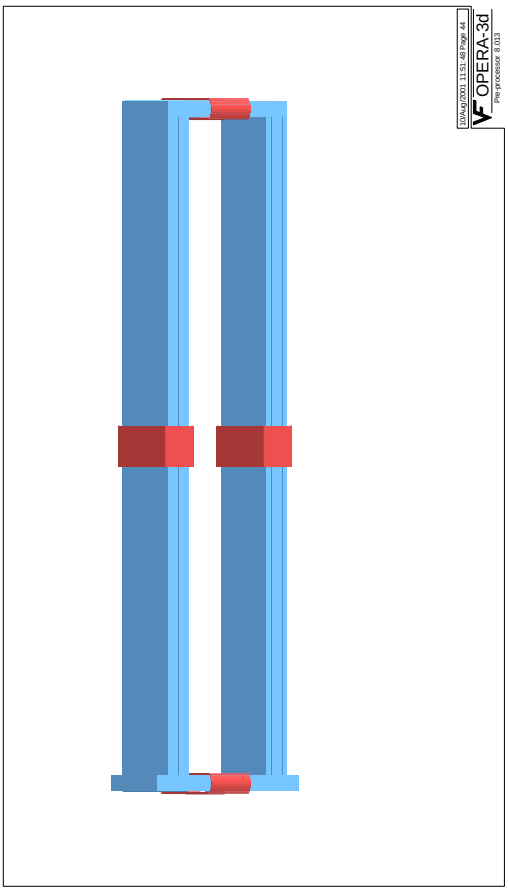

Figure 21: TOSCA model for the prototype with four coils.

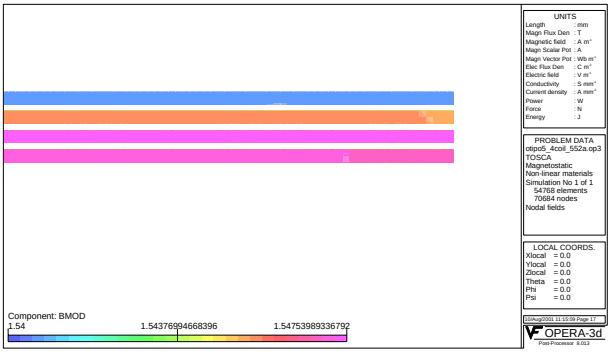

Figure 22: Field in iron at the pick-up coil.

References

[1] The OPERA collaboration, M. Guler et al., CERN/SPSC 2000-028, SPSC/P318, LNGS P25/2000.

[2] OPERA note in preparation

[3] OPERA-3d OPERA-2d and TOSCA are products by Vector Field Ltd., Oxford, UK (www.vectorfields.co.uk)